Novel Uniaxial Force Sensor based on Visual Information for Minimally Invasive Surgery

A. Faragasso, J. Bimbo, Y. Noh, A. Jiang, S. Sareh, H. Liu, *Member, IEEE*
T. Nanayakkara, H.A. Wurdemann and K. Althoefer, *Member, IEEE*

Abstract— This paper presents an innovative approach of utilising visual feedback to determine physical interaction forces with soft tissue during Minimally Invasive Surgery (MIS). This novel force sensing device is composed of a linear retractable mechanism and a spherical visual feature. The sensor mechanism can be adapted to endoscopic cameras used in MIS. As the distance between the camera and feature varies due to the sliding joint, interaction forces with anatomical surfaces can be computed based on the visual appearance of the feature in the image. Hence, this device allows the measurement of forces without introducing new stand-alone sensors.

A mathematical model was derived based on validation data tests and preliminary experiments were conducted to verify the model's accuracy. Experimental results confirm the effectiveness of our vision based approach.

I. INTRODUCTION

In recent years, Minimally Invasive Surgery (MIS), also called laparoscopic or keyhole surgery, has become a well-established and preferred approach to a growing number of major surgeries ranging from relatively simple procedures such as prostatectomy [1], cholecystectomy [2], and cystectomy [3] to more complex surgical operations which are very difficult to conduct laparoscopically such as coronary artery revascularization and mitral valve repair [4] [5]. MIS procedures are performed using instruments that are inserted via 12-15 mm incisions called Trocar ports which allow surgeons to bring surgical tools and sensors into the patient's body. MIS offers a number of advantages over traditional open surgery including improved therapeutic outcome, shortened postoperative recovery, reduced immunological stress response of the tissue and tissue trauma, and less postoperative pain; MIS is also is cost-effective [6]. However, it is reported that the absence of physical tissue interaction is a major limitation of MIS compared to traditional open surgeries [7]. During open procedures, surgeons have direct access to soft tissue of organs and are able to manually palpate. Surgeons can directly investigate the force-displacement response to

A. Faragasso, J. Bimbo, Y. Noh, S.Sareh, H. Liu, T. Nanayakkara, H.A. Wurdemann and K. Althoefer are with the Centre for Robotics Research, Department of Informatics, King's College London, London, WC2R 2LS, UK `angela.faragasso, joao.bimbo, yohan.noh, allen.jiang, sina.sareh@kcl,hongbin.liu, thrish.antha, helge.wurdemann, k.althoefer@kcl.ac.uk`
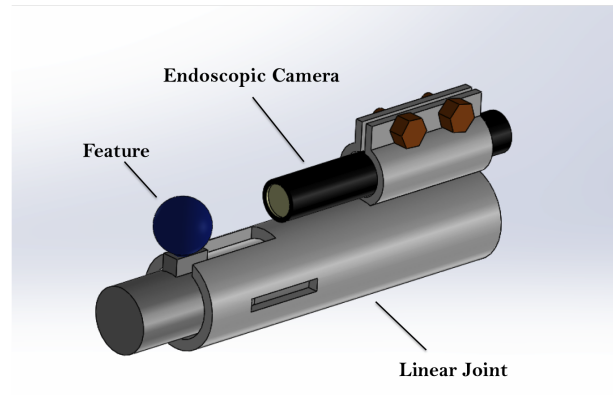
Fig. 1: Novel Vision-based Single Axial Force Sensor (CAD Drawing)

acquire distributed tactile information. Hence, haptic (force and tactile) feedback has become essential in MIS: In palpation procedures for tumor localization, clinicians press their fingers on the patient's anatomical surfaces to assess tool-tissue interaction forces to diagnose tissues as normal or abnormal using tactile feedback [8]. Tissue areas that are stiffer than the surrounding tissue can be recognized as potentially abnormal and tumourous for instance [9]. Since surgical robotic devices are improving incisively the performance of the operations, they have been developed beyond the investigational stage. Currently, these device continue to evolve as they become more ergonomic [10]. Although vision has been improved in MIS through the introduction of high-definition 2D and 3D vision systems, methods of direct palpation and haptic feedback in MIS are still in their infancy. The force applied to soft organs can only be estimated through visual feedback by observing the deformation of the tissue in the transmitted camera images. Performing safe surgeries in limited space and dynamic environments where surgeons have a restricted view and no sense of touch have created a growing demand on surgical vision techniques and sensor developments in order to retrieve tactile feedback similar to traditional open surgery. Analysis shows that a new design is required to address these problems that occur with the current equipment [7].

We propose a new low-cost vision-based force sensing device as shown in Figure 1. The paper is organised as follows: Section II reviews the current state of the art in sensing approaches for MIS. The design of the proposed sensing portotype is described in Section III. Section IV presents

the real-time visual algorithm and initial vision-stress tests. From this, the mathematical model is derived (Section V). The experimental results are reported in Section VI.

II. BACKGROUND

Trejos et al. [11] reviewed the current state of the art in force sensing technologies in order to underline the current limitations and evaluate the benefits of haptic information for surgical tasks in MIS. Recently, a number of sensors have been developed to address the issue of force feedback for keyhole surgery. In order to provide surgeons with haptic feedback, researchers have integrated surgical instruments with sensing capability to feed back the sense of touch when indenting or grasping soft tissue [12]. One approach of force measurements is to use light modulation techniques. In [13], a miniaturized fiber optic sensor suitable for MR-guided cardiac catheterization uses the variation in distance and orientation between a reflective surface and a fiber optic cable to estimate the axial and lateral force applied on a surgical tip while the orientation is retrieved through image analysis. The same principle was used to develop the triaxial force sensor in [14]. This device can compute the orthogonal component of the force applied to a compliant structure. A distal force sensor suitable for minimally invasive tissue palpation was developed in [15]. This sensor uses the optical fibre principle to compute the tissue interaction force and can measure forces in a range of $3\,\mathrm{N}$ in axial and $1.5\,\mathrm{N}$ in radial direction. In [16], elastomer elements were used to develop an MR-compatible uniaxial force sensor for mitral valve annuloplasty utilised within a beating heart. It is waterproof and electrically passive. In [17] and [18], an indentation depth sensor was developed and tested during a rolling indentation procedure. The wheeled device can compute tissue reaction forces as well as identify tissue stiffness distribution visualised in form of a stiffness map. A robotic master-slave teleoperated system with force reflection capabilities that can be incorporated in MIS was developed in [19]. The haptic master interface can reflect forces in all directions. On the slave side, an actuation mechanism and force/torque sensors were used within a disposable tip.

So far, tactile and force sensors have been applied to surgical tools in MIS to measure local tissue properties. Providing this feedback supports the surgeon operating with remote mechanisms. Many studies use commercially available force sensors such as the ATI Nano17 to measure force and torque accurately. However, constraints on size, geometry, costs, bio-compatibility and sterelisability make some of these approaches not suitable for MIS. In [20], a force sensor was integrated with the tip of an existing robotic instrument for instance considerably increasing costs. Hence, another research direction is to estimate forces applied to soft tissue without using any traditional stand-alone force sensors.

Due to the limitations of the above technologies, this paper proposes a new low-cost vision-based force sensing device as shown in Figure 1. The advantages of this method are:

1) The sensor is small in size and can be miniturised for MIS.

2) The current fabrication of the device provides MR-compatibility, water and corrosion resistance, and leads to a lightweight sensing structure.
3) The sensor principle is based on feature tracking combining vision and a spring mechanism. The work takes inspiration from the method used for wheeled robot navigation in [21].
4) The sensing range and resolution can easily be customised by changing the inside spring. "Softer" springs enable high force resolution sacrificing range and *vice-versa*.

The presented device can be attached to an endoscopic camera allowing to measure forces along one 1 axis during MIS procedures.

III. VISION-BASED FORCE SENSOR DESIGN

The prototype of the developed sensory device is shown in Figure 2. Figure 2(a) gives an overview of the disassembled parts. The camera spring force sensor consists of a spring-driven linear shaft which is inserted into a cylindrical housing in order to prevent lateral movement of the compression spring. A small body (here: a spherical feature) is used to "visualize" interaction forces. This assembled mechanism is attached to a vision system as it can be seen in Figure 2(b).
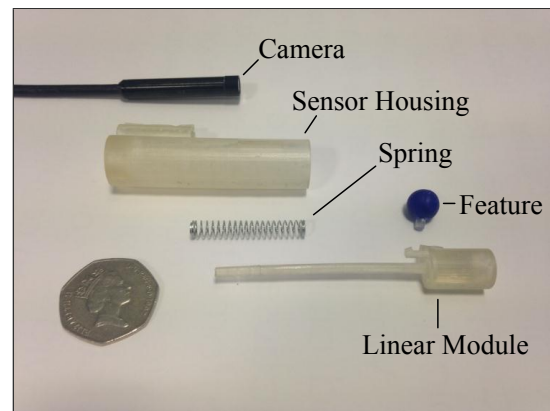
(a)
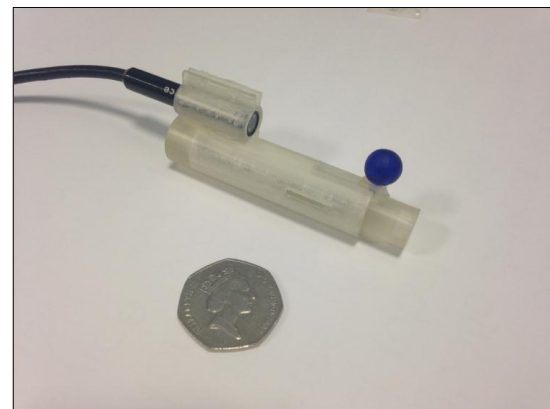
(b)

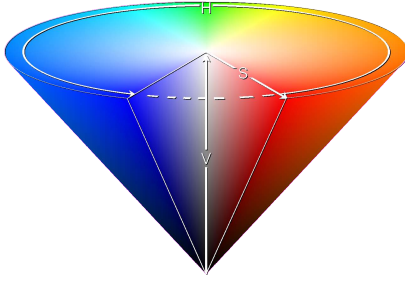Fig. 2: (a) Disassembled and (b) Assembled Force Sensor Prototype

Fig. 3: HSV Colour Space

The design allows the feature to be in the field of view of the camera. As the sphere interacts with soft tissue, the distance between the camera and end-effector is modulated.

The size of the sensor is compared to a 50 pence sterling coin. The spherical feature has a diameter of $5\,\mathrm{mm}$, the spring length is $35\,\mathrm{mm}$ and the linear shaft is $15\,\mathrm{mm}$ long. The used camera is a USB camera with an outer diameter of $7\,\mathrm{mm}$, resolution of $640\mathrm{x}480$ and a frame rate of $30\,\mathrm{frames/s}$. The feature can be mounted directly on the linear sliding shaft or on the end-effector having direct contact with the surrounding objects. The model was designed using SolidWorks and manufactured with a rapid prototyping machine (Project HD-3000 Plus, 3D Systems). The Project rapid prototyping machine employs a large number of printing jets to print objects in 3D. Using this machine to manufacture the novel sensing mechanism allows miniaturisation.

The resolution and range of this design are customisable, depending on the spring constant of the inner spring. The maximum force the sensor can measure is limited by the maximum size of the spring that can be integrated with a laparoscopic tool that fit through a Trocar port. The resolution is variable, as it depends on the current distance between the camera and the feature. It corresponds to the minimum observable change in force, which is the required force to increase the radius of the tracked feature by 1 pixel. This value is larger when the feature is further away from the camera and decreases as it comes closer.

IV. INTRINSIC RELATION BETWEEN VISUAL FEEDBACK AND FORCE

A. Real-time Image Processing

Image processing is performed using OpenCV, an open source computer vision system interfaced in ROS (Robot Operating System). It is based on the detection and tracking of a colored sphere in an image. Here, we use the HSV colour channel for colour detection. The HSV colour space is a model that describes a colour (Hue-value) in terms of its shade (Saturation or amount of gray) and brightness (intensity value or luminance). In its cylindrical representation (see Figure 3), the angle around the z-axis corresponds to the Hue value, the distance to the z-axis to the Saturation value which defines the colour's impurity and purity, and

the distance along the z-axis to the intensity (V value). A script was created to select the feature's HSV values. This allows to determine the colour interval online and adapt the algorithm in case of different feature colours.

For initial tracking, OpenCV's implementation of the Hough Transform is utilised to detect the feature. The performance of this method results in an inaccurate recognition as the feature is not able to be detected as a perfect circle. This effect occurs due to light disturbances in the environment affecting thresholds of the Canny edge detector which is performed intrinsically. To overcome this problem, a more sophisticated algorithm is implemented. Our method applies the morphological operator in a black/white image to select equivalent pixels in the HSV interval. Thus, it is possible to define the properties of areas in the image. Inner fragmentary regions are filled and bays along the corners eliminated. This is obtained through a sequence of two morphological primitives: dilate and erode. Noise and false positives affecting the HSV filter are removed using the Gaussian blur algorithm. Hence, the algorithm successfully detects the
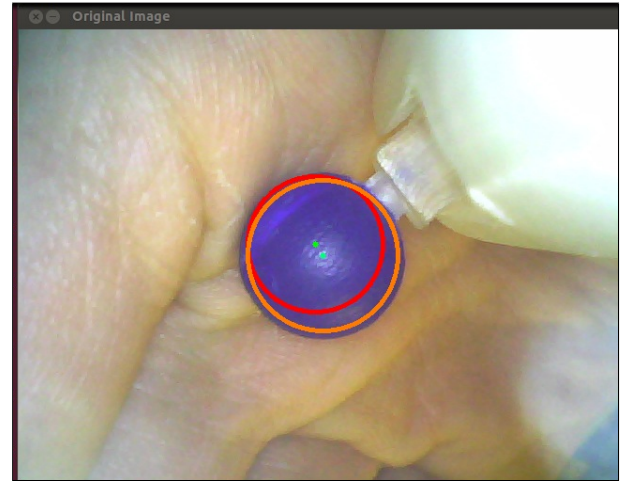

Fig. 4: Feature Detection using OpenCV HoughCircle (in red) and the proposed Algorithm (in orange)
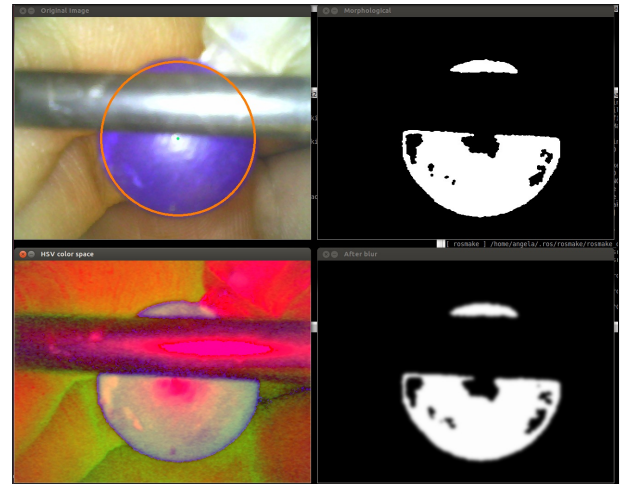

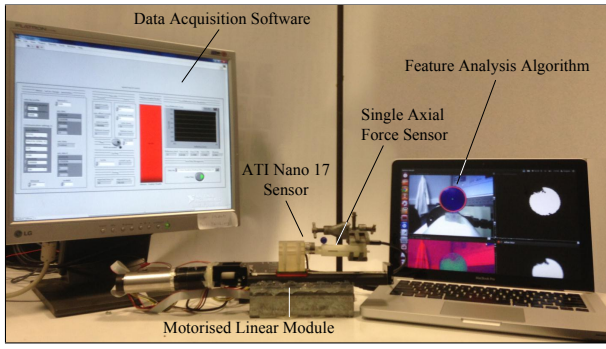Fig. 5: Vision Performance during Occlusions

Fig. 6: Setup

Fig. 8: Pinhole Camera Model

minimum enclosing circle that contains the white points in the image.

Figure 4 shows the comparison between the HoughCircle transformation and the improved algortithm. The performance difference can be clearly observed between the red and orange feature detection result. The developed algorithm is also robust to occlusions as shown in Figure 5. The image in the bottom left illustrates the transformation of the input image into HSV colour space. In the top right image, the output of the morphological operation and, in the bottom right image, the blurred image is shown. The field of view is occluded, however, the orange circle represents the successful feature detection in the top left image. This algorithm allows to accurately compute the radius of the feature which will be mapped to any applied force.

B. Computation of the Spring Parameter

In this section, stress test are performed using a ATI Nano 17 force/torque sensor (SI-12-0.12, resolution $0.003\,\mathrm{N}$ with a 16-bit data acquisition card) to validate the proposed method and determine the stability of the system. During the experimental tests, the device is fixed on a motorised linear module. The ATI Nano17 sensor applies linear forces to the feature while moving along the module. The force
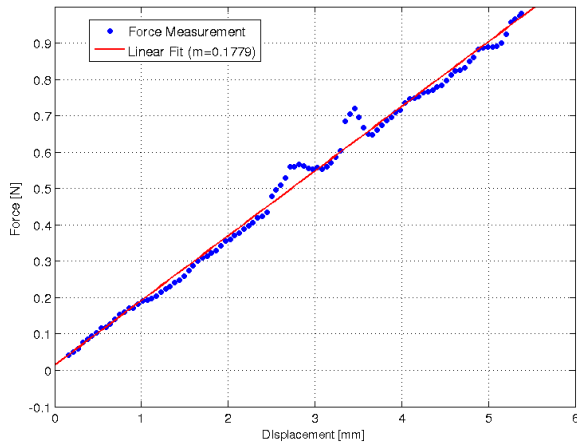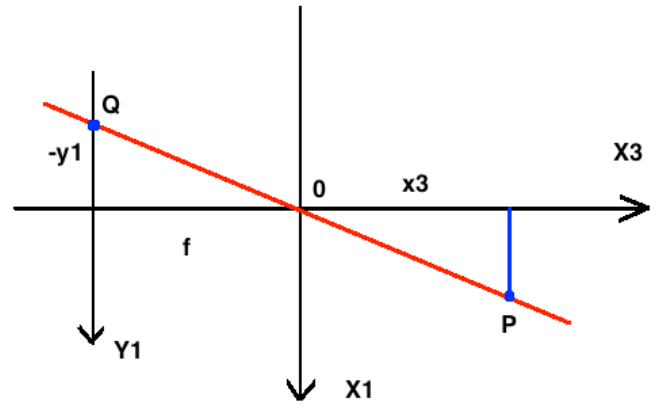

Fig. 7: Distance versus Force

sensor is connected to a PC running the LabView software in order to compute the spring constant. Image data is simultaneously recorded during this test. Figure 6 shows the entire experimental setup.

Figure 7 shows the results. The spring constant, that defines the relation between the displacement and the force, is equal to $177.9\,\mathrm{N/m}$ and was computed using a linear fitting.

V. MODELLING FORCE VERSUS FEATURE RADIUS

A. Mathematical Model

The pinhole camera model in Figure 8 defines the mathematical relationship between 3D point coordinates and their projection onto an image plane of an ideal pinhole camera. This ideal model can be used as a first order approximation of mapping a 3D scene to a 2D image. In this model, the focal length f represents the distance between the origin $\mathbf{O}$ of a 3D coordinate system and the image plane. Considering a point $\mathbf{P}$ in the world coordinate frame at $\mathbf{P} = (x_1, x_2, x_3)$ and its projection $\mathbf{Q} = (y_1, y_2)$ in the camera frame, it is possible to define the relation between the 3D coordinate of $\mathbf{P}$ and the coordinates of $\mathbf{Q}$ in (Y_1, Y_2) as shown in Figure 8. From the proprieties of the similar triangles, it follows that:

$$\begin{pmatrix} y_1 \\ y_2 \end{pmatrix} = -\frac{f}{x_3} \begin{pmatrix} x_1 \\ x_2 \end{pmatrix} \tag{1}$$

We considered the relation between the sphere dimension into the 2D image and the distance computed by the sensor during the contact. As the feature has a spherical shape and the embedded sensor allows movements only along a single axis that is perpendicular to the camera, the variation of sphere's radius in the image can be related to the distance. If r represents the sphere's radius, x the distance between the sphere position and the camera, and h the projection of the radius in the image plane, the following will result considering Equation 1:

$$\frac{h}{x} = \frac{r}{f} \tag{2}$$

Considering the initial position x_0 and radius r_0 of the sphere, from Equation 2 is possible to express every new
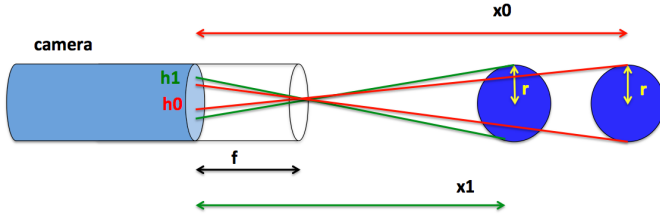
Fig. 9: Sphere's Projection in the Image Plane

position in function of these known variables, shown in Figure 9:

$$x = \frac{hf}{r} = \frac{x_0 r_0}{r} \quad (3)$$

We obtain the expression of Δx:

$$\Delta x = x_0 - \frac{r_0}{r} x_0 \quad (4)$$

The model that expresses force in function of the circle radius was obtained using Equation 4 in Hooke's law for the force response of springs:

$$F(r) = K x_0 \left(1 - \frac{r_0}{r}\right) \quad (5)$$

Here, K represents the spring constant. The initial position of the spherical feature x_0 is equal to $42\,mm$ and the initial radius r_0 is 94 pixels. The mathematical model depends on the design of the sensor and the visual feature, i.e. initial radius r_0 and feature-camera distance x_0, so an adjustment is required for any new design of the sensor. In addition, the sphere's radius can be substituted with other geometrical parameters and this make its validation independent of the visual feature shape . To evaluate the performance of the model, the Root Mean Squared Error (RMSE) was used which is defined as:

$$\text{RMSE} = \sqrt{\frac{\sum_{t=1}^{n} (y - F(r))^2}{n}} \quad (6)$$

The resulting RMSE for this model was 0.0404. Figure 10 plots the results of the experimental data and the mathematical model. It can be seen that the model does not fit exactly with the experimental data.
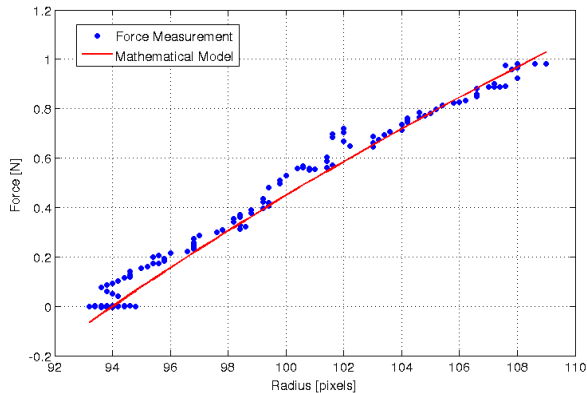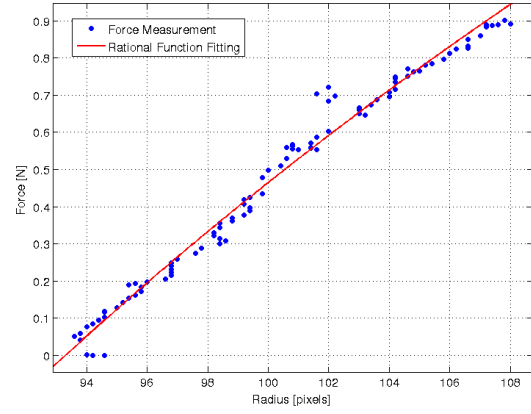

Fig. 11: Experimental Model Fitting

B. Experimental Model

The next approach is to find a mathematical function that directly expresses forces measured in terms of the feature's radius. This equation is derived using Matlab's Curve Fitting Tool, where the best fit to the data points is found. Figure 11 shows the fitted curve which is obtained using the rational function in Equation 7. Since the mathematical model was derived in the previous section, there is no risk of overfitting.

$$F(r) = a_1(1 - \frac{a_2}{r}) \quad (7)$$

The parameters found were a_1= 7.143 and a_2=91.94. The fit has a prediction interval of $95\,\%$ and its RMSE is 0.03.

VI. EXPERIMENTAL RESULTS

Experimental tests were performed to validate the models described on the previous two sections. Our sensor was manually pushed against the Nano 17 force/torque sensor. The results in Figure 12 shows that both models perform reasonably well, failing only when the force goes above the sensors range, which is lower than the benchmarking sensor, saturating it. Another issue was the response speed of the sensor, which is affected by the existence of friction.
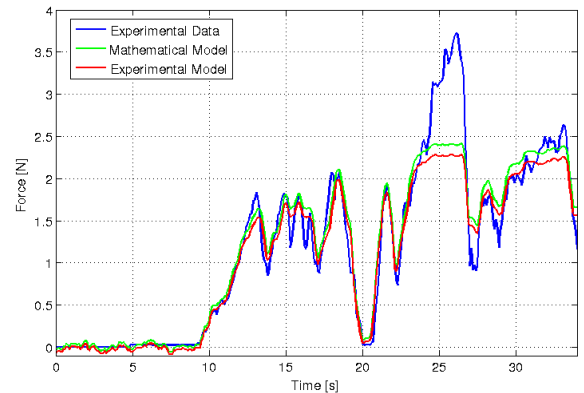

Fig. 10: Mathematical Model Fitting

Fig. 12: Model Results

Since the desired application of this sensor is MIS, very fast response speed is not an essential requirement. In terms of accuracy when the force is inside the sensor's range, the RMSE was 0.1535 for the mathematical model and, for the experimental model 0.1355.

The spring used in this experiment allowed a range of $0 - 1.96$ N and a variable resolution between 0.0439 N and 0.0787 N.

VII. DISCUSSION AND CONCLUSIONS

In this paper a new force sensor mechanism has been proposed which utilises visual information to compute force exerted by tracking a feature. The sensor consist of a normal camera and a compression spring, and can be used in combination with an endoscopic camera. The resulting device is, therefore, low-cost and can be regarded as a disposable instrument. Here, we have explained our approach for the design and the implementation of a new sensing device which, to the best of authors' knowledge, is the first implementation of force sensing device which only relies on visual information. In this work, we have also developed an image tracking algorithm that relates the radius of the spherical feature into the values of the exerted force. This tracking algorithm can be generalised to be used with various geometries of the feature. In order to validate our design and modelling approach we have obtained the force-radius relationship through experiments. The experimental results shown that the mathematical model derived presents a good approximation of the experimental data obtained through benchmarking with a very accurate commercial force sensor. The limitations and inaccuracies of the sensor are mostly due to lens distortion and friction. These issues should be addressed in future designs. Further development of this sensing device will also consider miniaturisation and optimisation studies on the size and the geometry of the visual feature. Problems that can effect the performance of the vision algorithm, i.e. occlusions due to blood and smoke will also be regarded investigating new kind of materials and vision processing algorithms.

REFERENCES

[1] T. Wilson and R. Torrey, "Open versus robotic-assisted radical prostatectomy: which is better?," *Current Opinion in Urology*, vol. 21 (3), pp. 200–205, 2011.

[2] W. Ji, Z. Zhao, J. Dong, H. Wang, F. Lu, and H. Lu, "One-stage robotic-assisted laparoscopic cholecystectomy and common bile duct exploration with primary closure in 5 patients," *Surgical Laparoscopy Endoscopy Percutaneous Techniques*, vol. 21 (2), pp. 123–126, 2011.

[3] P. Zehnder and I. S. Gill, "Cost-effectiveness of open versus laparoscopic versus robotic-assisted laparoscopic cystectomy and urinary diversion," *Current Opinion in Urology*, vol. 21 (5), pp. 415–419, 2011.

[4] M. E. Currie, J. Romsa, S. Fox, W. Vezina, C. Akincioglu, J. Warrington, R. McClure, L. Stit, A. Menkis, W. Boyd, and B. Kiaii, "Long-term angiographic follow-up of robotic-assisted coronary artery revascularization," *The Annals of Thoracic Surgery*, vol. 93 (5), p. 142631, 2012.

[5] S. Masroor, C. Plambeck, and M. Dahnert, "Complex repair of a barlows valve using the da vinci robotic surgical system," *ISOs Work on Guidance for Haptic and Tactile Interactions*, vol. 19 (5), p. 593595, 2010.

[6] J. Whynott, "Micro Molding: Meeting the Challenges of Designing Medical Devices for MInimallu Invasive Surgery," in *2008 Micro/Nano Conference & Exhibits Society of Manufacturing Engineers*, no. 313, 2008.

[7] M. van Veelen, E. Nederlof, R. Goossens, C. Schot, and J. Jakimowicz, "Ergonomic problems encountered by the medical team related to products used for minimally invasive surgery.," *Surg Endosc*, vol. 17, no. 7, pp. 1077–81, 2003.

[8] T. R. Coles, D. Meglan, and N. W. John, "The role of haptics in medical training simulators: A survey of the state of the art," *IEEE Transactions on Haptics*, vol. 4, no. 1, pp. 51–66, 2011.

[9] H. Stassen, J. Dankelman, and C. Grimbergen, "Developments in Minimally Invasive Surgery and Interventional Techniques (MISIT)," *Conference on human decision making and manual control*, pp. 212–218, 1997.

[10] D. M. Herron and M. Marohn, "A consensus document on robotic surgery.," *Surgical endoscopy*, vol. 22, pp. 313–25; discussion 311–2, Feb. 2008.

[11] A. L. Trejos, R. V. Patel, and M. D. Naish, "Force sensing and its application in minimally invasive surgery and therapy: a survey," *Proceedings of the Institution of Mechanical Engineers, Part C: Journal of Mechanical Engineering Science*, vol. 224, pp. 1435–1454, Jan. 2010.

[12] G.-P. Haber, M. A. White, R. Autorino, P. F. Escobar, M. D. Kroh, S. Chalikonda, R. Khanna, S. Forest, B. Yang, F. Altunrende, R. J. Stein, and J. H. Kaouk, "Novel robotic da vinci instruments for laparoendoscopic single-site surgery," *Urology*, vol. 76, no. 6, pp. 1279 – 1282, 2010.

[13] P. Polygerinos, P. Puangmali, T. Schaeffter, R. Razavi, L. D. Seneviratne, and K. Althoefer, "Novel miniature mri-compatible fiber-optic force sensor for cardiac catheterization procedures," in *Robotics and Automation (ICRA), 2010 IEEE International Conference on*, pp. 2598–2603, IEEE, 2010.

[14] P. Puangmali, P. Dasgupta, L. D. Seneviratne, and K. Althoefer, "Miniaturized triaxial optical fiber force sensor for mri-guided minimally invasive surgery," in *Robotics and Automation (ICRA), 2010 IEEE International Conference on*, pp. 2592–2597, IEEE, 2010.

[15] P. Puangmali, H. Liu, L. D. Seneviratne, P. Dasgupta, and K. Althoefer, "Miniature 3-axis distal force sensor for minimally invasive surgical palpation," *IEEEASME Transactions on Mechatronics*, vol. 17, no. 4, pp. 1–11, 2011.

[16] M. C. Yip, S. G. Yuen, and R. D. Howe, "A robust uniaxial force sensor for minimally invasive surgery.," *IEEE transactions on biomedical engineering*, vol. 57, pp. 1008–11, May 2010.

[17] H. Liu, P. Puangmali, D. Zbyszewski, O. Elhage, P. Dasgupta, J. S. Dai, L. Seneviratne, and K. Althoefer, "An indentation depthforce sensing wheeled probe for abnormality identification during minimally invasive surgery," *Proceedings of the Institution of Mechanical Engineers, Part H: Journal of Engineering in Medicine*, vol. 224, pp. 751–763, June 2010.

[18] H. Liu, J. Li, X. Song, L. Seneviratne, and K. Althoefer, "Rolling indentation probe for tissue abnormality identification during minimally invasive surgery," *Robotics, IEEE Transactions on*, vol. 27, no. 3, pp. 450–460, 2011.

[19] M. Tavakoli, R. V. Patel, and M. Moallem, "A Force Reflective Master-Slave System for Minimally Invasive Surgery," no. October, pp. 3077–3082, 2003.

[20] U. Seibold, B. Kubler, and G. Hirzinger, "Prototype of instrument for minimally invasive surgery with 6-axis force sensing capability," *Robotics and Automation, . . .*, no. April, pp. 498–503, 2005.

[21] N. Alt, Q. Rao, and E. Steinbach, "Haptic exploration for navigation tasks using a visuo-haptic sensor," in *Interactive Perception Workshop, ICRA 2013*, (Karlsruhe, Germany), May 2013.